

Recent Results from Thunderstorm electrification modeling

E. R. Mansell¹, D. R. MacGorman², J. M. Straka³, C. L. Ziegler²

¹CIMMS, University of Oklahoma, Norman, Oklahoma, U.S.A.

²National Severe Storms Laboratory, Norman, Oklahoma, U.S.A.

³School of Meteorology, University of Oklahoma, Norman, Oklahoma, U.S.A.

ABSTRACT: The recently upgraded OU/NSSL thunderstorm electrification model now includes an explicit treatment of small ion processes and other improvements. Sensitivity experiments find a wide range of electrical and lightning characteristics for the same storm but with different charge separation parameterizations. The same microphysical/dynamical evolution can, depending on the choice of charge separation parameterizations (both noninductive and inductive), produce very different lightning behavior. For example, a storm might produce CG lightning of either or both polarities or none at all (intracloud lightning only).

Introduction

The three dimensional storm model with detailed microphysical parameterizations provides self-consistent distributions of charges in a thunderstorm environment. There are 12 bulk hydrometeor categories (cloud droplets, rain, three ice crystal habits, aggregates, three graupel densities, frozen drops, and small and large hail), each with an associated charge density. The branched lightning parameterization of *Mansell et al.* [2002] is used with an electric field initiation threshold that decreases exponentially with increasing altitude (the runaway or breakeven threshold). Small ion processes such as attachment and drift motion are treated explicitly following *Chiu* [1978] and others, and a parameterization of surface corona emission is included. Corona emission occurs when the vertical component of the surface electric field exceeds a magnitude of 5 kV m^{-1} .

The model includes five parameterizations of non-inductive graupel-ice charge separation. The ‘Gardiner/Ziegler’ (Gard) scheme comes from *Ziegler et al.* [1991], with an adjustable reversal temperature T_r . (Here $T_r = -15^\circ\text{C}$, so that graupel gains negative charge for $T < -15^\circ\text{C}$.) Two parameterizations utilize the idea of the critical rime accretion rate RAR_{crit} that divides positive and negative charging regions (Fig. 1). The first is the ‘Riming Rate’ (RR) parameterization, which is based on *Brooks et al.* [1997] with modifications to the critical rime accretion rate (RAR) curve following *Saunders and Peck* [1998] and the charging results for smaller cloud droplets in *Saunders et al.* [1999]. The second RAR -based scheme is from *Saunders and Peck* [1998] (SP98) with the RAR_{crit} curve stretched toward lower temperatures (Fig. 1). The parameterization of the results from *Takahashi* [1978] (Taka) follows *Helsdon et al.* [2001] with the addition of a factor to vary the charge separation per collision based on impact velocity and crystal size [*Takahashi*, 1984]. The last scheme is from *Saunders et al.* [1991] (S91) with modifications of *Helsdon et al.* [2001] that drastically reduces charge separation at low effective liquid water content.

Inductive charging is parameterized for rebounding graupel-droplet collisions as in *Ziegler et al.* [1991]. The efficiency or strength of the inductive charging is controlled by the rebound rate E_r and average cosine of impact angle of rebounding droplets $\langle \cos \theta \rangle$. Three inductive charging strengths are used here: off (no inductive charging), moderate (mod) ($E_r = 0.007$, $\langle \cos \theta \rangle = 0.2$), and strong (str) ($E_r = 0.015$, $\langle \cos \theta \rangle = 0.5$).

The multicell thunderstorm has an analytical thermodynamic sounding and half-circle hodograph [*Weisman and Klemp*, 1984]. The hodograph arc length is $U_s = 20 \text{ m/s}$ (0-5 km shear = $2U_s/\pi$) and

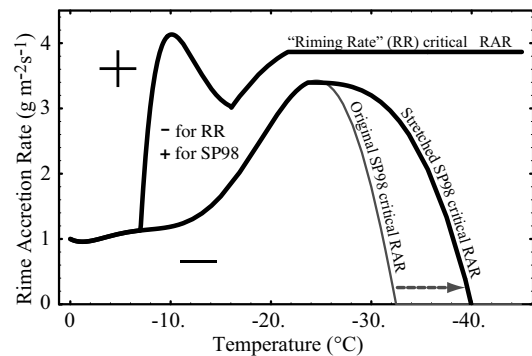


Figure 1: Critical RAR curves for the RR and SP98 noninductive charging parameterizations. Graupel gains positive charge for $RAR > RAR_{\text{crit}}$.

the boundary layer vapor mixing ratio is 13.5 g kg^{-1} . Simulations were performed in a 45-km by 45-km by 18-km domain with constant horizontal spacing of 500 m and vertical spacing that stretched from 200 m at the ground to 500 m aloft. The storm was initiated with a warm bubble with randomized thermal perturbations. Each case was run for at least two hours, by which time almost all convection had decayed. Because there is no feedback from the electrification to the dynamics, each case has identical dynamics and microphysics. The model is initialized with a profile of positive and negative small ions to produce a ‘fair weather’ electric field profile.

As is always the case with models, a number of factors could affect the results. The representation of ice crystal size and number density, especially for $T > -15^\circ\text{C}$, can have a large effect on the noninductive charging parameterizations that have a strong size dependence. Also, graupel-graupel collisions are currently not treated, largely because of the lack of laboratory data on charge separation between two larger particles.

Results

The sensitivity study of *Helsdon et al.* [2001] was an important step in the use of models to test the results of graupel-ice crystal charge separation in the laboratory. The present model greatly expands upon *Helsdon et al.* [2001]: a 3-D model instead of 2-D, inclusion of lightning so that a complete life cycle can be simulated, and greater number of combinations of charge separation parameterizations. The five noninductive charge separation parameterizations were each run three times with the different settings for inductive charging, for a total of 15 simulations. Table 1 summarizes the lightning produced by each combination. For all five sets of runs, there were no CG flashes at all when inductive graupel-droplet charging was turned off. The number of IC flashes was slightly reduced for moderate inductive charging, suggesting an overall discharging effect, as was found with lower-strength inductive charging by *Ziegler et al.* [1991]. Significant numbers of CG flashes were produced only with the stronger inductive charging parameters. The total number of IC flashes varied by an order of magnitude from 57 for S91/mod to 672 for Gard/str.

| Charging Scheme | Number of Flashes | | |
|-----------------|-------------------|-----|-----|
| | IC | +CG | -CG |
| RR/off | 153 | 0 | 0 |
| RR/mod | 139 | 1 | 0 |
| RR/str | 405 | 5 | 1 |
| Gard/off | 392 | 0 | 0 |
| Gard/mod | 344 | 0 | 0 |
| Gard/str | 672 | 0 | 18 |
| Taka/off | 141 | 0 | 0 |
| Taka/mod | 123 | 0 | 1 |
| Taka/str | 424 | 0 | 26 |
| SP98/off | 126 | 0 | 0 |
| SP98/mod | 125 | 0 | 0 |
| SP98/str | 385 | 5 | 1 |
| S91/off | 70 | 0 | 0 |
| S91/mod | 57 | 0 | 0 |
| S91/str | 247 | 1 | 3 |

Table 1: Summary of total lightning for each simulation. See text for details on noninductive/inductive charging details. Totals are shown for 120 minutes elapsed time from model initiation.

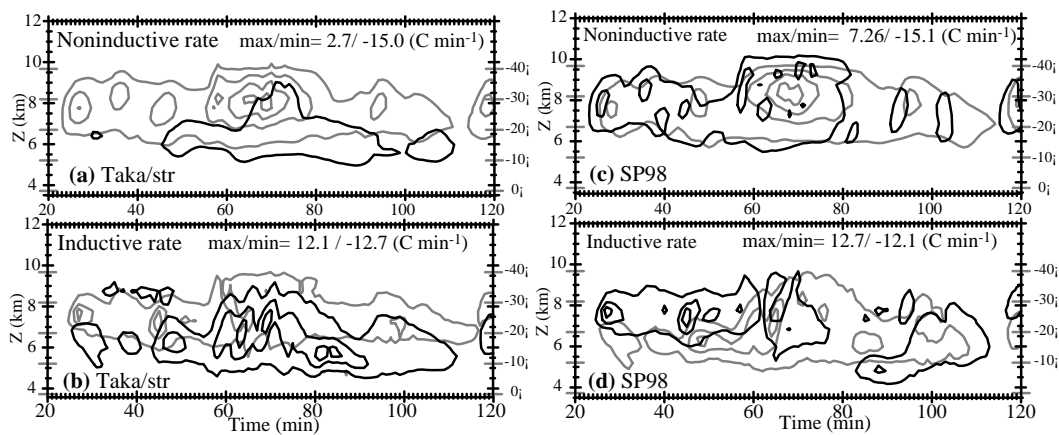


Figure 2: Noninductive and Inductive horizontally integrated charging rates per model level as functions of time and height for Taka/str (a,b) and SP98/str (c,d). The lowest contour line is 1 C min^{-1} with intervals of 4. Gray contours are negative charge to graupel, black contours show positive charge transferred to graupel.

The Gard/str and Taka/str schemes had similar results. Both produced many –CG flashes and had similar lightning characteristics. Fig. 2(a,b) shows the positive and negative graupel charging rates due to noninductive and inductive charge separation for the Taka/str. (Note that the noninductive charge sep-

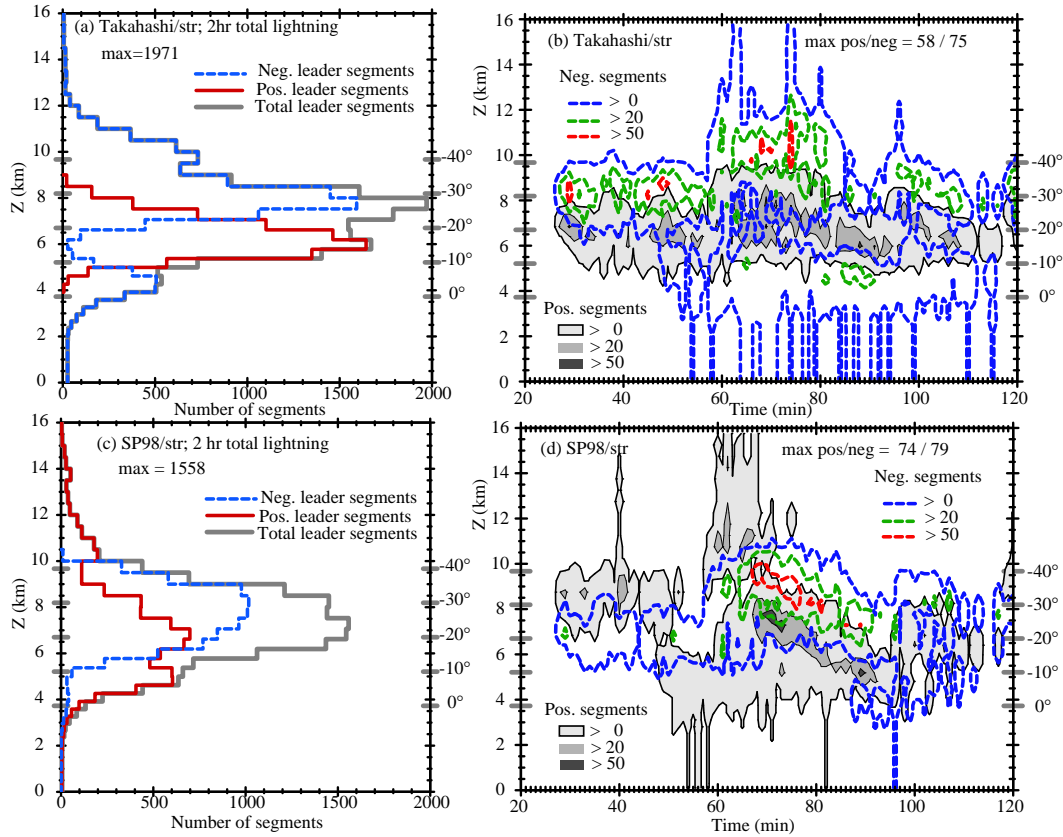


Figure 3: Lightning characteristics for Taka/str and SP98/str simulations. (a,c) Lightning leader segments by height summed over 2 hr. (b,d) Time-Height contours of lightning leaders summed by height over 1-min intervals.

aration is independent of the inductive charging.) By itself, the Taka scheme would not provide enough positive charging of graupel at lower levels to develop a strong lower positive charge (LPC). The strong inductive setting allows a positive feedback to occur, generating regions of significant charge not found in the noninductive-only cases. In Fig. 2(b) the positive inductive charging at 6–7 km increases after 45 min. This occurs as graupel and meltwater rain are recycled into a new updraft, providing precipitation ice particles and thus charge separation at lower levels. The mid-level negative charge region is also enhanced by the upward-carried, negatively charged droplets. This process causes sufficiently large electric field magnitudes for lightning flashes to initiate between the LPC and midlevel negative regions, some of which reach ground to become –CG flashes.

The *RAR*-based schemes (RR and SP98) both had initially positive noninductive charge transfer to graupel [Fig. 2(c)] because of the high liquid water contents in the initial updrafts (and thus high *RAR*). The result is a charge structure of midlevel positive charge with upper-level negative charge. Comparing Fig. 2(b) and (d) shows a near mirror-image of the inductive charging through about 60 min. In the SP98 case, the precipitation recycling and inductive charging processes generate a lower *negative* charge region that results in +CG flashes. Eventually the charging structure (and lightning, Fig. 3) becomes more like Taka/str case.

Sample lightning characteristics are shown in Fig. 3 for the Taka/str and SP98/str cases. Positive and negative leader segments are horizontally integrated and shown as totals for the 2 hr simulation and as time-height contours. The time-height contours of lightning reflect the radical

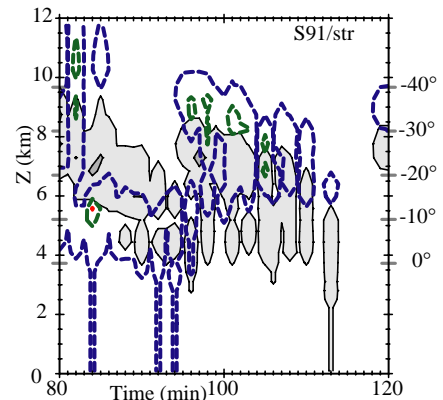


Figure 4: As in Fig. 3(b) but for the last 40 minutes of the S91 case.

changes in the time-height contours of lightning reflect the radical

difference between the charging schemes during the first 40–50 min. The Taka/str simulation initially produces a main negative/upper positive charge dipole, resulting in IC flashes with upward negative leaders and downward positive leaders. The SP98/str simulation, however, initially produces ‘inverted’ IC lightning with upward positive/downward negative leaders, indicating generally opposite charge structure. The single –CG flash in the SP98/str case was preceded by positive inductive charging at 5-km altitude ([Fig. 2(d)].

The +CG flash in the S91/str simulation was the last lightning flash from a decaying cell (Fig. 4). It initiated in the forward flank region of the decaying storm and was preceded by a series of IC flashes (‘normal’ polarity) at steadily decreasing altitude. Negatively charged precipitation is falling out of the storm, weakening the mid-level negative charge region and causing more favorable conditions for the flash to reach ground. It is not clear what factors are involved in a flash going to ground, and the model probably underpredicts the overall rate of CG flashes. As in *Mansell et al.* [2002], all +CG flashes were initiated between a positive charge region with a negative charge region underneath.

As expected, flash rates are correlated with graupel and updraft volume (Fig. 5). The SP98/str case has initially lower flash rates than the Taka/str because of competition between positive and negative noninductive charging. The peak SP98/str flash rate at 70 min coincides with strong negative charging of graupel both non-inductively and inductively.

Conclusions

The model results indicate that graupel recycling combined with inductive graupel-droplet charge separation could be an important process in the development of some CG flashes. It may help explain why low-precipitation (LP) supercells generally produce few –CG flashes: The large wind shear associated with LP storms may cause graupel to be carried too far from the updraft for much recycling to occur, thus hindering the development of a strong LPC and possibly promoting +CG flashes from the forward flank.

Acknowledgments

Support was provided by NSSL and NSF grants ATM-9617318 and ATM-9807179, and ATM-0119398. Funding for this research also was provided under NOAA-Univ. of Oklahoma Cooperative Agreement NA17RJ1227.

References

- Brooks, I. M., C. P. R. Saunders, R. P. Mitzeva, and S. L. Peck, The effect on thunderstorm charging of the rate of rime accretion by graupel, *Atmos. Res.*, *43*, 1997.
- Chiu, C.-S., Numerical study of cloud electrification in an axisymmetric, time-dependent cloud model, *J. Geophys. Res.*, *81*, 5025–5049, 1978.
- Helsdon, J. H., Jr., W. A. Wojcik, and R. D. Farley, An examination of thunderstorm-charging mechanisms using a two-dimensional storm electrification model, *J. Geophys. Res.*, *106*, 1165–1192, 2001.
- Mansell, E. R., D. MacGorman, C. L. Ziegler, and J. M. Straka, Simulated three-dimensional branched lightning in a numerical thunderstorm model, *J. Geophys. Res.*, *107*, 10.1029/2000JD000244, 2002.
- Saunders, C. P. R., and S. L. Peck, Laboratory studies of the influence of the rime accretion rate on charge transfer during crystal/graupel collisions, *J. Geophys. Res.*, *103*, 13,949–13,956, 1998.
- Saunders, C. P. R., W. D. Keith, and R. P. Mitzeva, The effect of liquid water on thunderstorm charging, *J. Geophys. Res.*, *96*, 11,007–11,017, 1991.
- Saunders, C. P. R., E. E. Avila, S. L. Peck, N. E. Castellano, and G. G. A. Varela, Vapor and heat supply to riming graupel: Effect on charging, in *Preprints, 11th Intl. Conf. Atmos. Elec.*, pp. 268–271, ICAE, Guntersville, AL, 1999.
- Takahashi, T., Riming electrification as a charge generation mechanism in thunderstorms, *J. Atmos. Sci.*, *35*, 1536–1548, 1978.
- Takahashi, T., Thunderstorm electrification – a numerical study, *J. Atmos. Sci.*, *41*, 2541–2558, 1984.
- Weisman, M. L., and J. B. Klemp, The structure and classification of numerically simulated convective storms in directionally varying wind shears, *Mon. Wea. Rev.*, *112*, 2479–2498, 1984.
- Ziegler, C. L., D. R. MacGorman, J. E. Dye, and P. S. Ray, A model evaluation of non-inductive graupel-ice charging in the early electrification of a mountain thunderstorm, *J. Geophys. Res.*, *96*, 12,833–12,855, 1991.

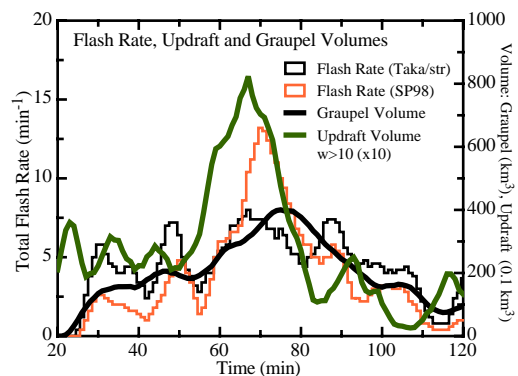


Figure 5: Graupel volume, updraft volume (scaled by a factor of 10) and total flash rates for the Taka/str and SP98/str cases (5-minute smoothing applied).